Electronic Supplementary Information (ESI)

Fe_3Pt Intermetallic nanoparticles anchored on N-doped Mesoporous Carbon for Highly Efficient Oxygen Reduction Reaction

Danke Chen, Zhuoyi Li, Yu Zhou, Xu Ma, Hanqing Lin, Wen Ying, Xinsheng Peng*

State Key Laboratory of Silicon Materials, school of Materials Science and Engineering, Zhejiang University, Hangzhou 310027, China.

Experiment Section

Chemicals

Zinc nitrate ($Zn(NO_3)_2 \cdot H_2O$), ferric nitrate ($Fe(NO_3)_3 \cdot 6H_2O$), ethanol (CH_3CH_2OH) and isopropanol ($(CH_3)_2CHOH$) were purchased from Sinopharm Chemical Reagent Co., Ltd. 2-aminoethanol (NH_2-CH_2CH_2OH) and Nafion solution (5 wt %) were obtained from Sigma-Aldrich. 2-methylimidazole (2-mIm), potassium chloroplatinate ($K_2[PtCl_4]$) and potassium hydroxide (KOH) were purchased from Aladdin. Commercial Pt/C (20wt%) catalyst was purchased from Johnson Matthey. All chemicals were used as received without further purification.

Synthesis of Fe_3Pt/N@C

For the synthesis of Pt-Fe@ZIF-8, Pt-Fe co-functionalized zinc hydroxide nanotrands (ZHNs) were initially prepared. Generally, 4 mM $Zn(NO_3)_2$ and 0.04 mM $Fe(NO_3)_3$ aqueous solution were mixed with 1.6 mM aminoethanol aqueous solution under stirring, with further aging at room temperature for 30 min to form Fe doped ZHNs.[1] Subsequently, 0.0133 mM $K_2[PtCl_4]$ aqueous solution was added to the as-prepared Fe doped ZHNs dropwise under vigorous stirring, forming a homogeneous suspension. Then the resultant Pt-Fe co-functionalized ZHNs were collected through filtration and further immersed in 25 mM 2-mIm ethanol-water (Volume ratio, 2:3) solution for 24 hrs. After that, Pt-Fe@ZIF-8 was obtained by filtering and washing by water and ethanol several times. Finally, the sample was transferred into a quartz tube and heated to 900 °C kept for 30 min at a heating rate of 2 ^oC/min in flowing nitrogen atmosphere. The obtained material was directly used as electrocatalyst without further treatment. As a contrast, the Pt/N@C catalyst was prepared with the same procedure except without adding Fe precursor, while the

Fe/N@C catalyst was similarly prepared without adding Pt precursor. Furthermore, catalysts with different proportions of Fe-Pt were also prepared by regulating the concentration of $Fe(NO_3)_3$ used in the preparation of MOF precursors.

Material characterization

The morphologies, structures and elemental analyses were characterized by scanning electronic microscopy (SEM, S-4800, Hitachi), transmission electron microscope (TEM, HT-7700, Hitachi; JEM 2100F, JEOL), Raman spectroscopy (LabRAM HR Evolution, Horiba Jobin Yvon) and X-ray diffraction (XRD) (XRD-7000, Shimadzu) with Cu Kα radiation. The specific surface area and pore size distribution of all the catalysts were determined by recording N_2 adsorption–desorption isotherms at 77 K applying the Brunauer-Emmett-Teller (BET) method with a Micromeritics specific area analyzer (Micromeritics, 3Flex, SN#340). The samples were also analyzed by X-ray photoelectron spectroscopy (XPS) (AXIS Supra, Kratos Analytical) using monochromatic Al Kα radiation. The binding energy was calibrated by means of the C 1s peak energy of 284.6 eV.

Electrocatalytic ORR activity measurements

The electrocatalytic ORR activity measurements were performed in a conventional three-electrode cell at room temperature on the CHI 760E electrochemical analyzer using WaveDriver 20 bipotentiostat (Pine Instrument Company, USA). A Hg/HgO reference electrode was employed as reference electrode. All potentials initially measured versus the Hg/HgO reference electrode were converted to Reversible Hydrogen Electrode (RHE) reference scale as follows: $E_{(RHE)} = E_{(Hg/HgO)} + 0.059*pH + 0.098$. A graphite rod was used as the counter electrode. A glassy carbon disk (5 mm in diameter) and a glassy carbon disk (5.5 mm in diameter) with a Pt ring (6.5 mm in inner diameter and 8.5 mm in outer diameter) were used as the working electrode in rotating disk

electrode (RDE) and rotating ring-disk electrode (RRDE) experiments, respectively. The catalyst ink was prepared by ultrasonically dispersing 4 mg of catalyst in 1 mL isopropanol-water solution (Volume ratio, 4:1) containing 16 μL of 5 wt% Nafion solution to form a uniform suspension. 10 μL ink of catalysts was dropped onto the 0.196-cm^2 glassy carbon disk before the RDE experiments, resulting in the catalyst loading of 0.2 mg cm^{-2}.

Cyclic voltammetry (CV) tests were carried out in N_2- or O_2-saturated 0.1 M KOH electrolyte with a scan rate of 50 mV s^{-1} and the potential range was between 0 and 1.2 V *vs.* RHE. The linear sweeping voltammetry (LSV) measurements were performed at different rotation speeds (from 400 to 2500 rpm) with a scan rate of 10 mV s^{-1}. The cyclic stability of catalysts was evaluated using accelerated stress tests (ASTs) by cycling the potential from 0.6 to 1.0 V *vs.* RHE in O_2-saturated 0.1 M KOH with a rotation speed of 1600 rpm. The methanol tolerance ability was evaluated by chronoamperometry at 0.60 V *vs.* RHE with a rotation speed of 1600 rpm before and after adding 50 mL methanol into 150 mL O_2-saturated 0.1 M KOH solution.

The apparent electron transfer number was calculated from the Koutecky-Levich plots on the basis of Koutecky-Levich equation as follows:

$$\frac{1}{j} = \frac{1}{j_L} + \frac{1}{j_K} = \frac{1}{B\omega^{1/2}} + \frac{1}{j_K} \qquad (1)$$

$$B = 0.2nF\ {}_0D_0^{2/3}\gamma^{-1/6} \qquad (2)$$

where j, j_K and j_L are the measured, the kinetic and limiting current densities, respectively, ω is the electrode rotation rate, n is the electron transfer number, F is the Faraday constant (96485 C mol^{-1}), C_0 is the bulk concentration of O_2 in 0.1 M KOH (1.2×10^{-3} mol L^{-1}), D_0 is the diffusion coefficient of O_2 in 0.1 M KOH (1.9×10^{-5} cm^2 s^{-1}), and υ is the kinematic viscosity of the electrolyte (0.01 cm^2 s^{-1}).

The reaction order of dissolved oxygen was further calculated by plotting log(*j*) versus log(1-*j*/j_L) at various rotating rates as the following equation[2]:

$$\log j = \log j_k + m\log(1 - \frac{j}{j_L})$$

Where j_k was the kinetic current density, *m* was the reaction orders with respected to the dissolved oxygen. For the equation can be only employed for the reaction under kinetic-diffusion mixed control region, the corresponding plot at 0.7 V vs. RHE is chosen to show in Fig.S11b.

RRDE tests were conducted on the CHI 760E electrochemical analyzer at a rotation speed of 1600 rpm with a potential sweep of 10 mV s^{-1}; the Pt ring potential was set at 1.5 V *vs.* RHE. The electron transfer number (*n*) and the yield of hydrogen peroxide were obtained based on the following equation:

$$n = 4\frac{I_d}{I_d + I_r/N} \qquad (3)$$

$$H_2O_2\% = 200\frac{I_r/N}{I_d + I_r/N} \qquad (4)$$

where I_d and I_r are the disk current and ring current, respectively, and *N* is the collection efficiency of the Pt ring (*N* = 0.37, as provided by the manufacturer).

References

[1] X. Peng, J. Jin, N. Kobayashi, W. Schmitt, I. Ichinose, *Chem. Commun.*, 2008, 16, 1904-1906.

[2] Chia-Chin Chang, Ten-Chin Wen, Hsien-Ju Tien, *Electrochim. Acta*, 1997, 42, 557-565.

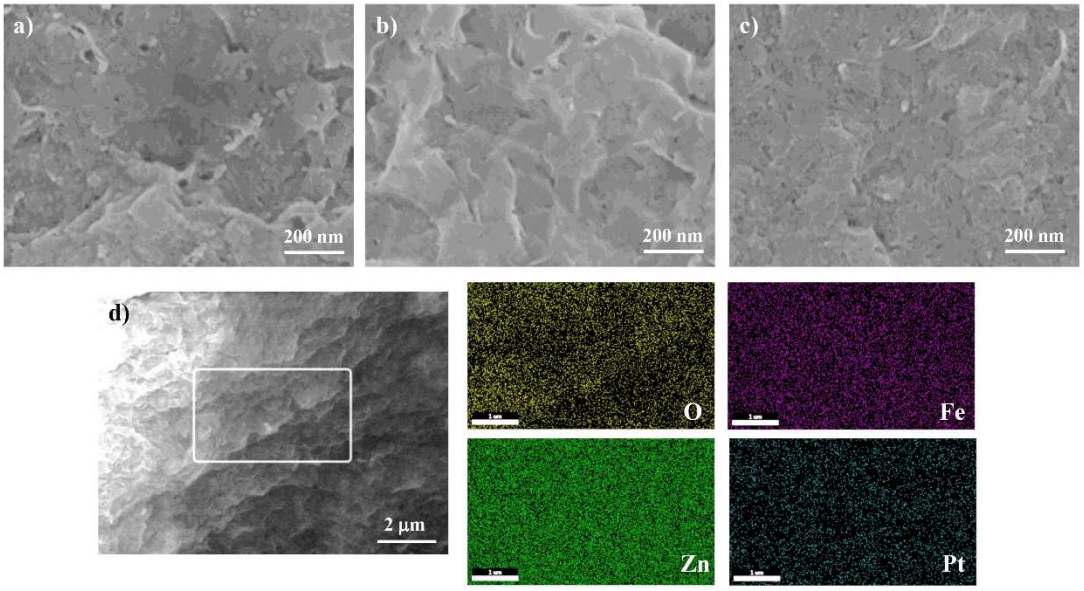

Fig. S1. SEM image of (a) Pt-Fe@ZHNs, (b) Pt@ZHNs, (c) Fe@ZHNs, (d) SEM image of Pt-Fe@ZHNs and the corresponding elemental mappings of the white square region marked in (d).

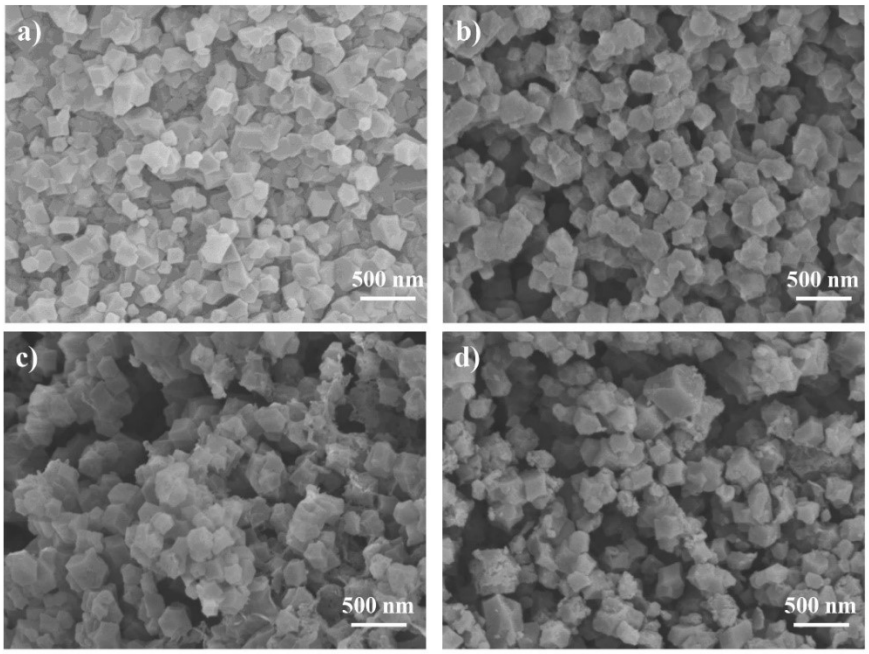

Fig. S2. SEM image of (a) ZIF-8, (b) Pt-Fe@ZIF-8, (c) Pt@ZIF-8, (d) Fe@ZIF-8.

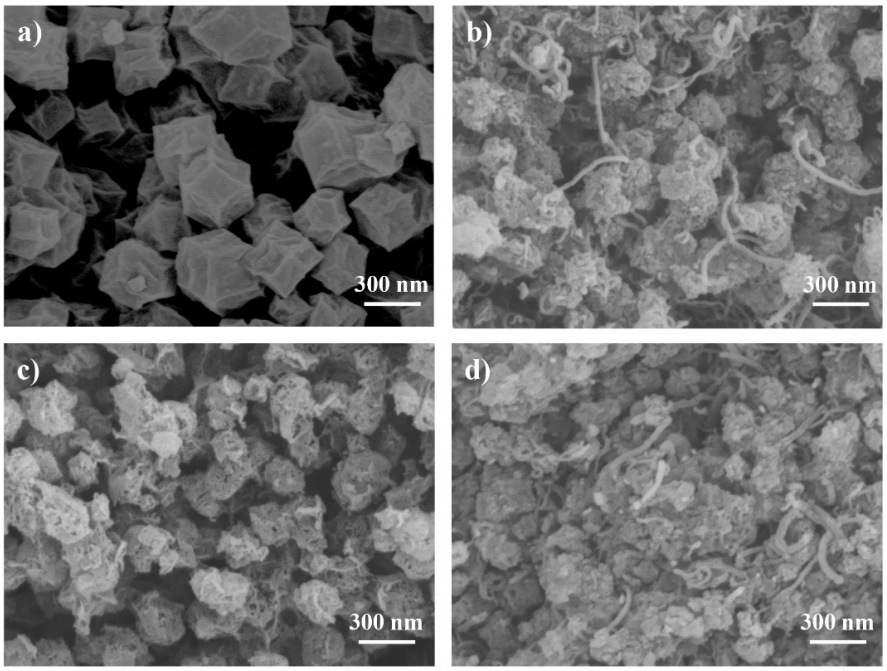

Fig. S3. SEM image of (a) N@C, (b) Fe_3Pt/N@C, (c) Pt/N@C, (d) Fe/N@C.

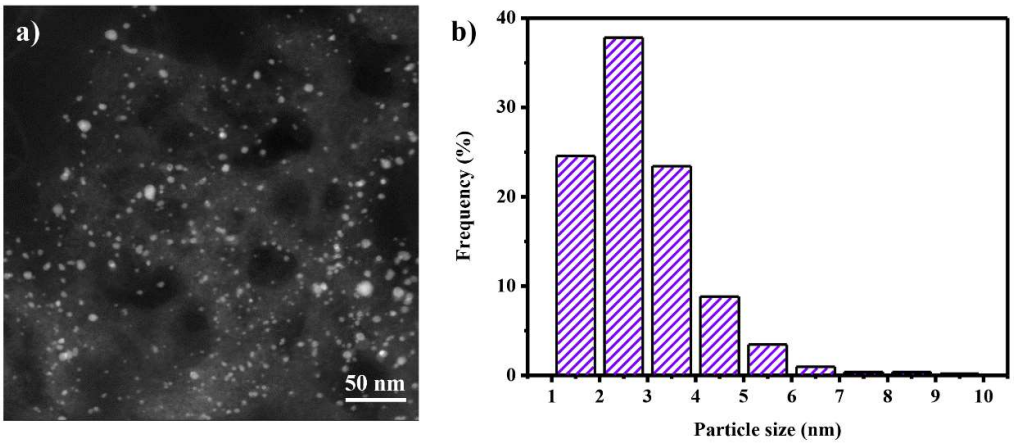

Fig. S4. (a) STEM image of Fe_3Pt/N@C, (b) Particle size distribution measured by STEM of more than 500 particles for Fe_3Pt/N@C.

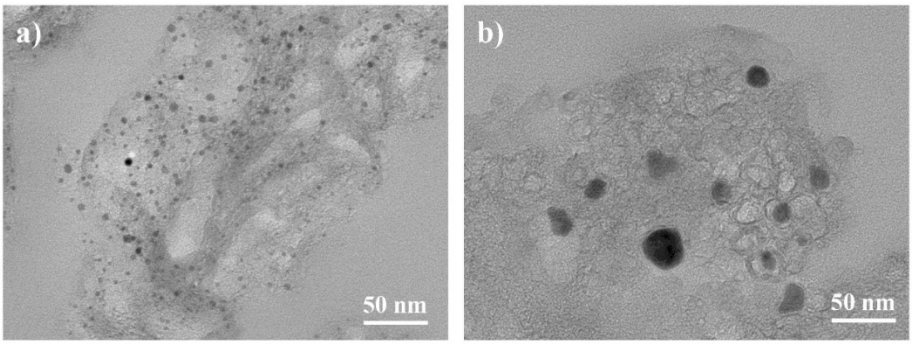

Fig. S5. TEM image of (a) Pt/N@C, (b) Fe/N@C.

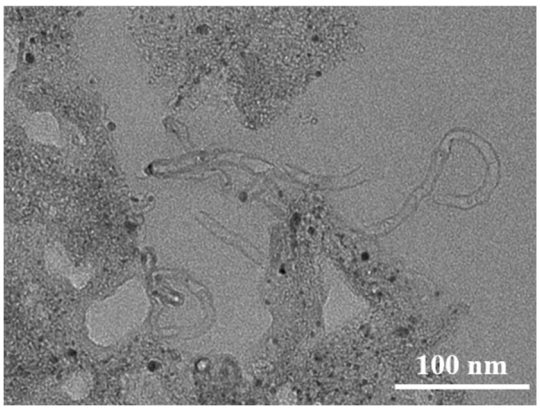

Fig. S6. TEM image of Fe_3Pt/N@C.

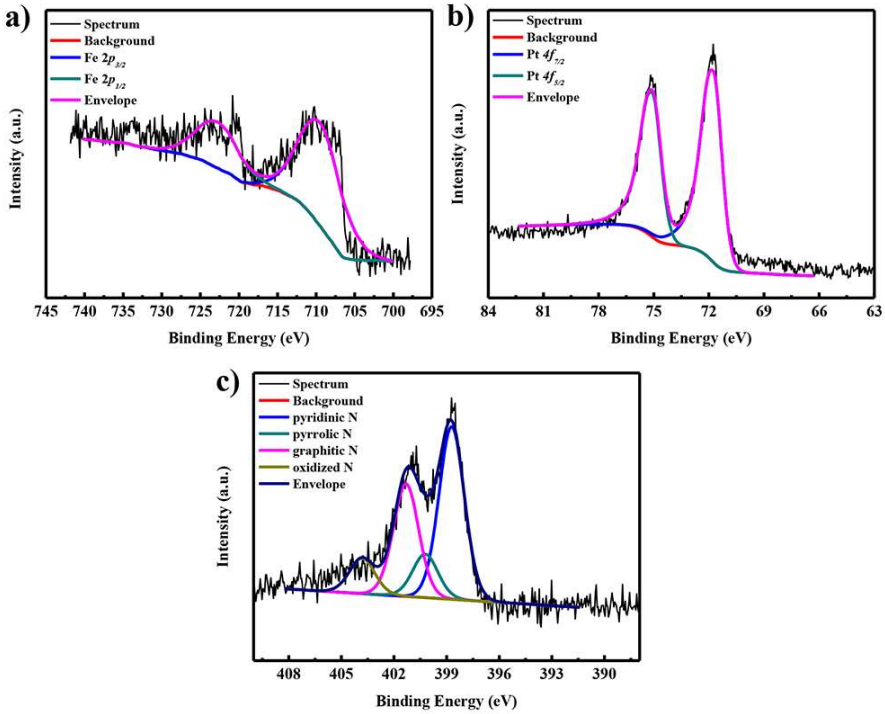

Fig. S7. The deconvoluted high resolution XPS scan of (a) Fe 2p; (b) Pt 4f; (c) N 1s of Fe_3Pt/N@C.

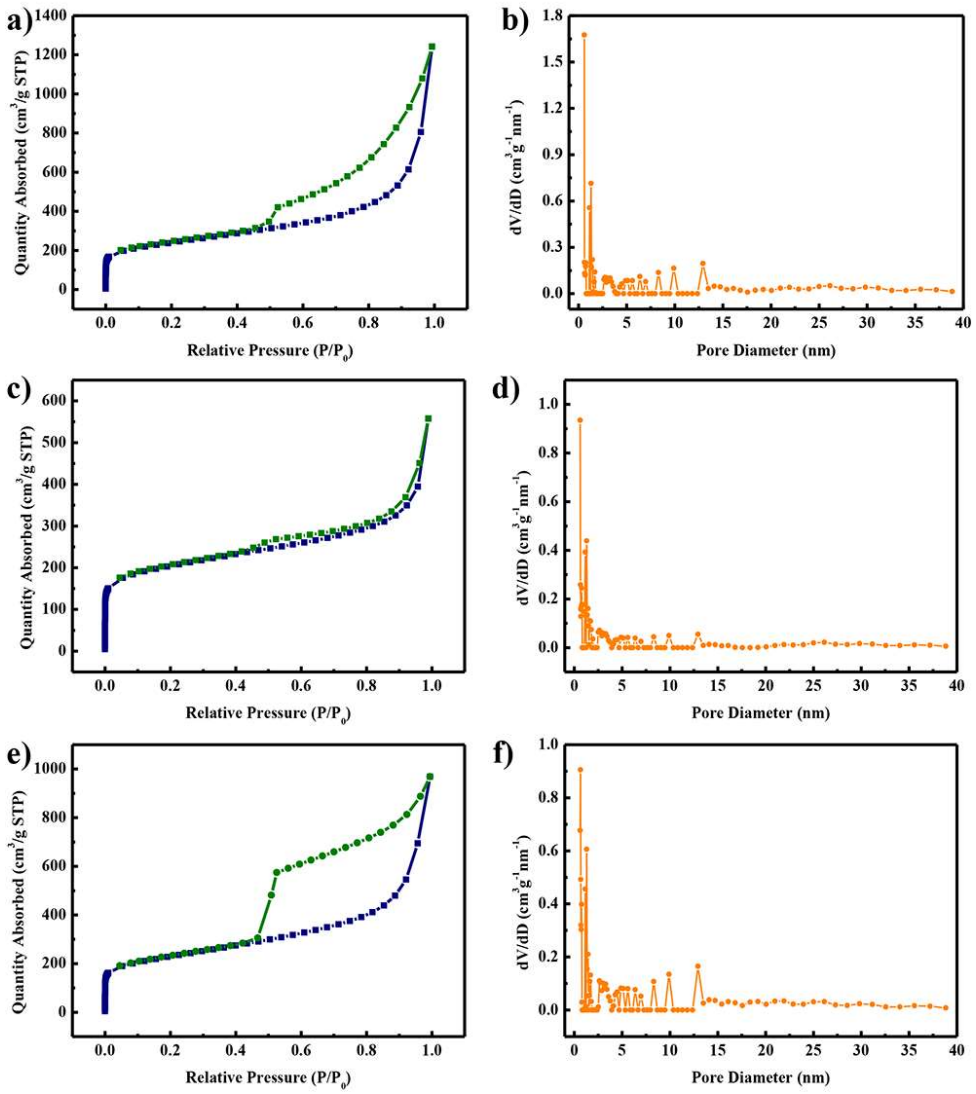

Fig. S8. Nitrogen adsorption–desorption isotherms of (a) Fe_3Pt/N@C, (c) Fe/N@C, (e) Pt/N@C; the corresponding DFT pore size distributions of (b) Fe_3Pt/N@C, (d) Fe/N@C, (f) Pt/N@C.

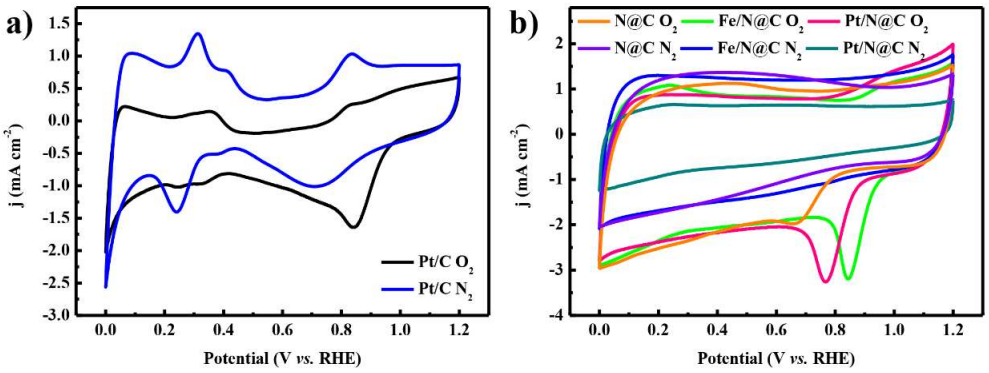

Fig. S9. CV curves of (a) commercial Pt/C, (b) Fe/N@C, Pt/N@C and N@C catalysts in O_2- or N_2- saturated 0.1 M KOH.

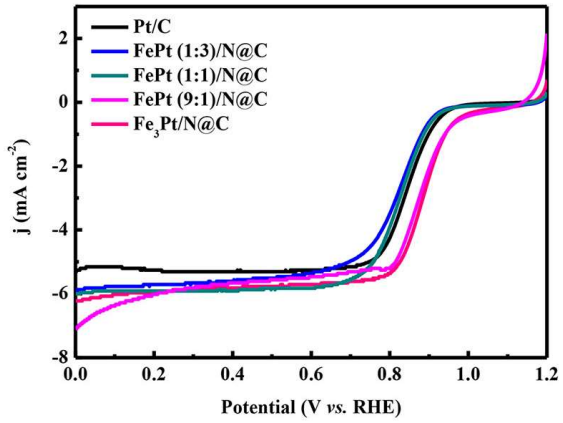

Fig. S10. LSV curves of catalysts of different compositions recorded in O_2-saturated 0.1 M KOH with a rotation rate of 1600 rpm.

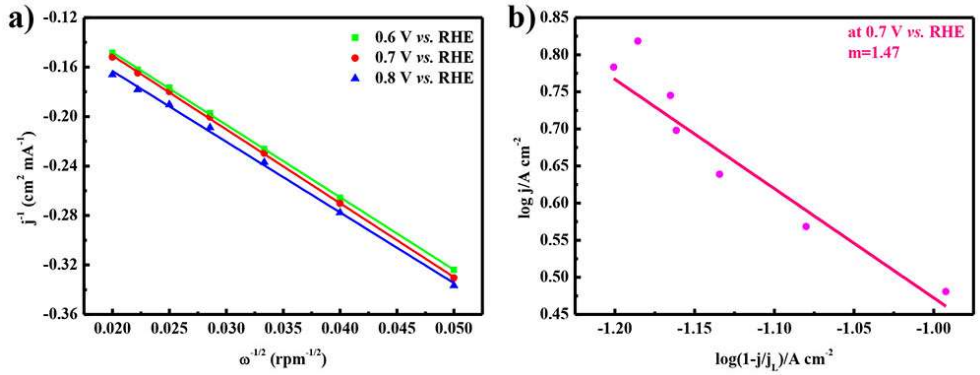

Fig. S11. (a) Koutecky-Levich plots of Fe_3Pt/N@C catalyst at different potentials; (b) Reaction order plot at 0.7 V vs. RHE for the O_2 reduction.

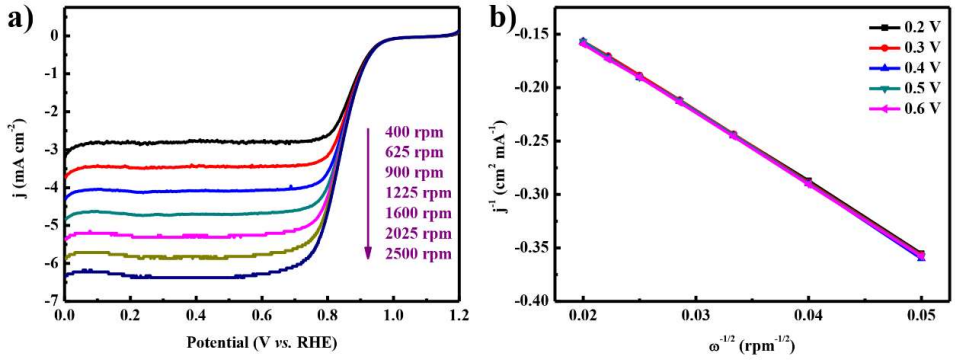

Fig. S12. (a) LSV curves of commercial Pt/C at different rotation rates of 400, 625, 900, 1225, 1600, and 2025 rpm; (b) the corresponding Koutecky–Levich plots at different potentials.

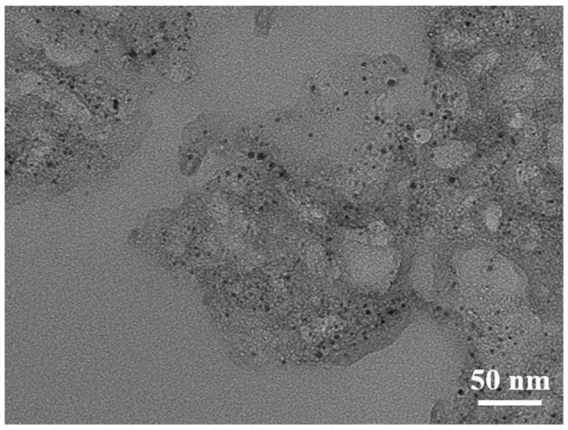

Fig. S13. TEM image of Fe_3Pt/N@C after 5000 CV cycles.

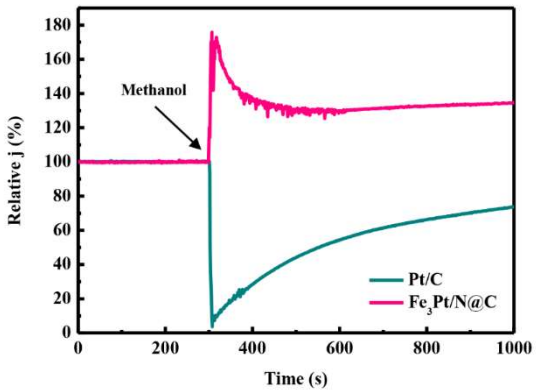

Fig. S14. Chronoamperometric response of the Pt/C and Fe_3Pt/N@C catalysts at 0.53 V in O_2 saturated 0.1 M KOH solution with the addition of 50 mL of methanol.

Table S1. A survey of the catalytic performances of various ORR electrocatalysts from recent literatures in alkaline solution.

No.	Catalysts	$E_{1/2}$	$\Delta E_{1/2}$*	Ref.
1	Pt-Ni@PC900	0.909	9	*ACS Omega,* 2020, 5, 2123-2132
2	FeNi/N-CPCF-950	0.864	16	*Appl. Catal. B: Environ.*, 2020, 263, 118344
3	Fe_7C_3/NG-800	0.85	10	*J. Colloid Interf. Sci.*, 2019, 556, 352-359
4	N-CNTs/ E-NNPs	0.86	-	*ChemCatChem*, 2019, 11, 4818-4821
5	$Fe_{1.6}$-N-HCNS/rGO-900	0.872	12	*ACS Nano*, 2018, 12, 5674-5683
6	Fe-ISA/SNC	0.896	55	*Adv. Mater.*, 2018, 30, 1800588
7	CoN_x/HCN-CNTs	0.92	20	*Appl. Surf. Sci.*, 2020, 504, 144380
8	Fe-NHPC-8	0.85	20	*J. Power Sources*, 2020, 448, 227443
9	G1000-ZC-2.0	0.885	30	*Carbon*, 2020, 156, 179e186182
10	Fe-N/C network	0.848	15	*Small Methods*, 2017, 1, 1700167
11	SA-Fe/NG	0.88	30	*PNAS*, 2018, 115, 6626
12	NS/C-950	0.85	-10	*Electrochim. Acta,* 2019, 318, 272e280276
13	FeNGC-T	0.88	40	*J. Mater. Chem. A*, 2019,7, 20132-20138
14	Fe_2C/CNFs	0.87	20	*Nanotechnology*, 2019, 30, 325403
15	Fe-N/GPC800	0.86	30	*ACS Appl. Mater. Interfaces* 2019, 11, 27823-27832
16	GL-Fe/Fe_5C_2/NG	0.86	20	*Adv. Energy Mater.* 2018, 8, 1702476
17	FeNC-900	0.837	10	*Nanoscale*, 2019, 11, 19506-19511
18	Fe/Fe_3C-NMC	0.88	20	*Electrochim. Acta*, 2019, 313, 255-260
19	NiCo/NC	0.84	-	*Carbon*, 2019, 155, 545e552
20	**Fe_3Pt/N@C**	**0.884**	**46**	**this work**

*: $\Delta E_{1/2} = E_{1/2}$ (catalysts)- $E_{1/2}$ (commercial Pt/C)